



Klinikum rechts der Isar

Technische Universität München



M.Sc in Biomedical Engineering and Medical Physics
Technical University of Munich

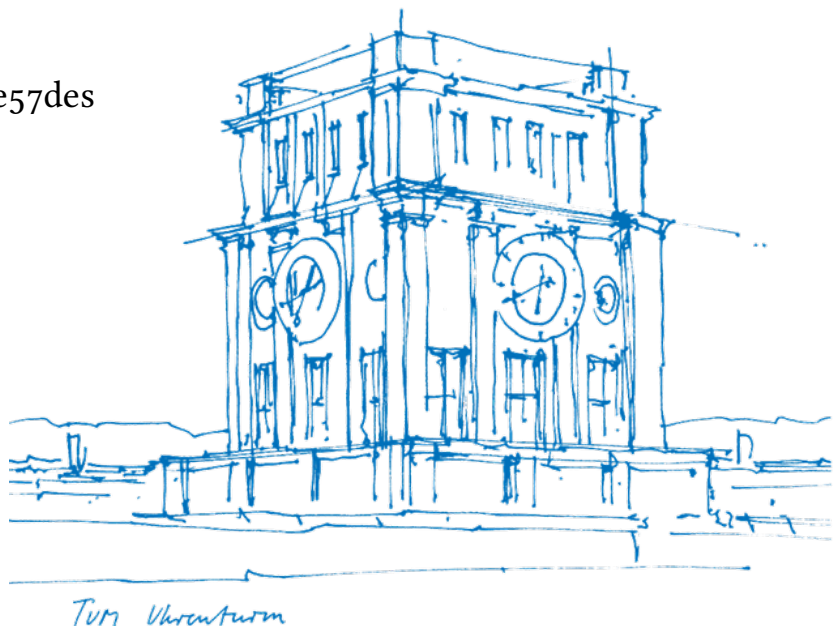
Robust Single Point Ultra Short Echo Time Water Fast Separation

Mateo Rodrigo Argudo Arrieta

Supervised by:
Prof. Dr. Dimitrios Karampinos
Anh Van Tu, PhD

Submitted by:
Mateo Argudo
Matriculation Number: ge57des

Submitted on:
May 15, 2024



DECLARATION

I hereby declare that the thesis submitted is my own unaided work. All direct or indirect sources used are acknowledged as references.

I am aware that the thesis in digital form can be examined for the use of unauthorized aid and to determine whether the thesis as a whole or parts incorporated in it may be deemed as plagiarism. For the comparison of my work with existing sources, I agree that it shall be entered into a database where it shall also remain after examination, to enable comparison with future theses submitted. Further rights of reproduction and usage, however, are not granted here.

This thesis was not previously presented to another examination board nor published.

Name: Mateo Rodrigo Argudo Arrieta

Date: asdasd

Place: Munich

ABSTRACT

Water–fat (WF) MRI is a set of techniques used in the assessment of metabolic dysfunction-related diseases. These techniques leverage the frequency shift between water and fat MR signals to separate them into two images, needing the acquisition of images at multiple echo times which extends the already prolonged MRI scan duration.

To shorten this acquisition time water-fat imaging has been combined with ultra-short echo time (UTE) techniques. The combination of these two methods are called UTE-Dixon imaging. These techniques have been used to suppress the fat signal in the MRI acquisitions and to determine tissue electron density properties. However, the need of two complex images to separate water and fat prolongs the scan time. A solution is to separate water and fat with the use of a single complex image instead of two, shortening scan time. This technique in combination with UTE acquisitions is called single-point UTE (sUTE) Dixon imaging. The use of a single image to separate water and fat introduces complexity to the problem, since some background phase contributions, coming from B_0 and B_1 field inhomogeneities cannot be implicitly deduced from only one echo. Hence, the problem becomes ill posed.

New techniques have arisen to tackle this problematic such as Kronthaler [citeKronthaler] with the use of a second order iterative optimization method (Gauss-Newton Method) with a smoothness constraint. Because the problem is ill posed initialization is necessary to ensure a proper convergence path and a better result of the water-fat separation.

This study aims to explore different methods to improve sUTE-Dixon imaging by addressing two different points:

1. Characteristics of background phase contributions and different approaches to modeling them.
2. How initialization techniques changes the behavior of the iterative optimization method results?.

We developed a sUTE-Dixon reconstruction framework based on the latest literature and integrated initialization techniques to further improve the method. This framework is used to compare reconstructions of different phantoms and anatomies with different hyper-parameters and initialization approaches.

Our findings reveal that initialization, not only prevents artifacts in reconstructed images but also significantly enhances the achievable water-fat separation quality. Additionally, we highlight two principal limitations of the current framework:

1. Its inability to accurately reconstruct water and fat at the anatomy/object edges.
2. Its sensitivity to mean phase shifts from the scan.

*We have seen that computer programming is an art,
because it applies accumulated knowledge to the world,
because it requires skill and ingenuity, and especially
because it produces objects of beauty.*

— **knuth:1974** [**knuth:1974**]

ACKNOWLEDGMENTS

Put your acknowledgments here.

Many thanks to everybody who already sent me a postcard!

Regarding the typography and other help, many thanks go to Marco Kuhlmann, Philipp Lehman, Lothar Schlesier, Jim Young, Lorenzo Pantieri and Enrico Gregorio¹, Jörg Sommer, Joachim Köstler, Daniel Gottschlag, Denis Aydin, Paride Legovini, Steffen Prochnow, Nicolas Repp, Hinrich Harms, Roland Winkler, Jörg Weber, Henri Menke, Claus Lahiri, Clemens Niederberger, Stefano Braglia, Jörn Hees, Scott Lowe, Dave Howcroft, José M. Alcaide, David Carlisle, Ulrike Fischer, Hugues de Lassus, Csaba Hajdu, Dave Howcroft, and the whole L^AT_EX-community for support, ideas and some great software.

Regarding L^AX: The L^AX port was initially done by *Nicholas Mariette* in March 2009 and continued by *Ivo Pletikosić* in 2011. Thank you very much for your work and for the contributions to the original style.

¹ Members of GuIT (Gruppo Italiano Utilizzatori di T_EX e L^AT_EX)



CONTENTS

I INTRODUCTION TO WATER FAT SEPARATION IN MRI

1	INTRODUCTION	2
1.0.1	Thesis Structure	4

II THEORY OF MAGNETIC RESONANCE IMAGING

2	MRI THEORY	7
2.1	Nuclear Magnetic Resonance (NMR)	7
2.1.1	Nuclear Spin and Magnetic Moment	7
2.1.2	Zeeman Effect	8
2.1.3	Bulk Magnetization	10
2.1.4	Resonance and RF Excitation	10
2.1.5	Relaxation Mechanisms	11
2.1.6	Chemical Shift	11
2.2	MRI Hardware Components	11
2.3	Spatial Encoding	11
2.3.1	Slice Selection	12
2.3.2	Frequency Encoding	12
2.3.3	Phase Encoding	12
2.3.4	k-Space and Image Reconstruction	12
3	WATER-FAT MRI	13
3.1	Importance of Water-Fat Separation	13
3.2	Chemical Shift Encoding (CSE)	13
3.3	Dixon Techniques	13
3.4	Applications in Clinical Diagnostics	13
4	CHALLENGES AND TECHNIQUES FOR ACCELERATION	14
4.1	Motion Artifacts	14
4.2	Respiratory Triggering and Breath-Hold Techniques	14
4.3	Compressed Sensing (CS)	14
4.3.1	Principles of Compressed Sensing	14
4.3.2	CS in MRI	14
4.3.3	CS in Water-Fat MRI	15
5	ADVANCED TECHNIQUES IN WATER-FAT MRI	16
5.1	Field Mapping	16

5.2	IDEAL Method	16
5.3	Graph Cut Algorithms	16
5.4	Conclusion	16
6	MATH TEST CHAPTER	17
 III APPENDIX		
A	APPENDIX TEST	19
 BIBLIOGRAPHY		
		20

LIST OF FIGURES

- Figure 2.1 Zeeman effect on an energy level for a nucleus with nuclear spin $I = 1/2$. The energy difference between the levels is half the Larmor frequency ω_L multiplied by \hbar . 9

LIST OF TABLES

LISTINGS

ACRONYMS

Part I

INTRODUCTION TO WATER FAT SEPARATION IN MRI

INTRODUCTION

Magnetic Resonance Imaging (MRI) is a fundamental tool in radiology and biomedical research, offering capabilities for both anatomical and functional imaging. MRI excels in providing superior soft-tissue contrast compared to CT scans and delivers higher resolution images than ultrasound, all while being a generally safe method with infrequent occurrences of patient harm [5] and no exposure to ionizing radiation.

MRI operates based on the Nuclear Magnetic Resonance (NMR) phenomenon to create changes in magnetization that are detectable by its receiver systems. It achieves spatial localization by stimulating nuclear spins within an external magnetic field. By modifying the imaging sequences, MRI can manipulate spin systems to produce various contrasts, such as relaxation, proton density, diffusion, and phase contrasts. Beyond producing diagnostic-quality images, MRI can also be adapted for quantitative analysis, which has spurred developments in creating maps of tissue physical properties for quantitative clinical interpretations.[4]

Globally, over 25,000 MRI scanners are in use, supporting a wide range of diagnostic and therapeutic applications. In neuroimaging, MRI is crucial for distinguishing between gray and white matter, aiding in the diagnosis of conditions like dementia, Alzheimer's disease, demyelinating diseases, epilepsy, and anomalies in the brain and spinal cord. It also facilitates diffusion and functional imaging techniques that can map neuronal tracts and blood flow. Cardiovascular uses of MRI include examining the structure and function of the heart and assessing vascular diseases. In musculoskeletal imaging, MRI is used for evaluating joints, spine, soft tissue tumors, and muscle disorders. Additionally, MRI is employed in abdominal assessments for the liver, gastrointestinal tract, breasts, and prostate, particularly useful in detecting cysts, tumors, and other abnormalities. Functional imaging of metabolites through spectroscopy is also a capability of MRI. [1]

In diagnostic imaging, fat presents a crucial MR signal component that often needs to be suppressed or differentiated from water signals. This manipulation is vital for accurate quantification of MR properties in tissues characterized by mixed chemical shifts. Particularly, imaging of short- T_2 tissues requires significant suppression of long- T_2 signals from both water and fat to enhance image contrast and clarity. The technology of water-fat (WF) imaging has evolved into state-of-the-art imaging methodology essential for differentiating between water and fat signals. These methods are particularly useful for qualitative purposes, such as suppressing the fat signal, or they are used quantitatively to derive biomarkers of tissue fat concentration such as the Proton Density Fat Fraction (PDFF). Furthermore, water-fat MRI is particularly useful for assessing diseases linked to metabolic disorders, such as obesity, metabolic syndrome, and type-2 diabetes [2, 3]. The ability to effectively manage fat signals in MRI is useful for improving the diagnostic accuracy of MRI scans and they not only provide a clearer visualization of anatomical structures but also facilitate a better understanding of tissue compositions, which is crucial for accurate diagnosis and treatment planning. [chapter]

This method utilizes chemical shift encoding (CSE) techniques, also known as Dixon imaging, capitalizing on the chemical shift differences between water and fat MR signals to differentiate them and create the two respective distinct images. The water-fat separation process involves fitting the acquired signal to a physical model, typically necessitating multiple image captures at different echo times. This requirement extends the scan duration, and coupled with the inherently slow MRI acquisition speed, increases the susceptibility of the technique to motion artifacts from patient or physiological movement. Techniques such as respiratory triggering or breath-hold are employed to minimize these artifacts, though they may elevate patient discomfort. Therefore, there is a pressing need to develop methods to expedite the MRI scanning process.

The challenge of prolonged scanning times in MRI is well-recognized, with a significant body of research focused on accelerating the acquisition process through fast sequences and parallel imaging techniques. Under this context multi-echo and single-echo ultra short echo time (UTE) sequences have been developed and studied to accelerate this scanning time [ute]. Specifically single-echo/single-point UTE Dixon techniques have been developed for fast acquisition with promising separation results since the short echo times make the R_2^* relaxation negligible; but it amplifies the relative effects of B_0 & B_1

field inhomogeneities affecting the quality of the water-fat separation, since the signal is not strong. Moreover, by using only one complex image the time dependent effects of the signal cannot be inferred, translating into a more complex that requires background phase corrections for a reliable WF separation.

Because of these pitfalls some techniques have been developed for single-point UTE Dixon like Kronthaler S., et. al [kronthaler], which use an iterative optimization method to solve the water-fat separation problem, trying to capture the background phase to remove it from the signal and continue with the classic separation algorithm. Although the algorithm tries to regularize the image by rewarding smoothness of the fitted phase, the problem is still ill posed and without proper initialization the stability of the algorithm may not deliver its full potential.

The purpose of this study is to analyze different modeling approaches of background phase contributions and various initialization techniques for the algorithm in Kronthaler S., et. al.; comparing it qualitatively with the non-altered model and studying its effects on the resulting water-fat separation quality and stability of the algorithm.

1.0.1 *Thesis Structure*

The thesis is organized into the following chapters:

- **Chapter 1:** The current chapter presents a brief introduction, motivation and purpose of the thesis.
- **Chapter 2:** Resumes the general theory of MRI, including physics theory, signal encoding, k-space and echo sequences.
- **Chapter 3:** Introduces the UTE sequences and the water fat separation of MRI signals.
- **Chapter 4:** Analyses the different background phase contributions and its effects in the resulting MRI acquisition.

- **Chapter 5:** Introduces the iterative optimization method used for water-fat separation and analyses the impact of different initialization strategies on its resulting water and fat images.
- **Chapter 6:** Summarizes the conclusions drawn from various results from the previous chapters.

Part II

THEORY OF MAGNETIC RESONANCE IMAGING

In this section we will introduce the theory of magnetic resonance imaging. We will start with the physics background in nuclear magnetic resonance, following to signal acquisition in k-space and signal encoding. Finally, echo sequences are introduced.

MRI THEORY

2.1 NUCLEAR MAGNETIC RESONANCE (NMR)

Nuclear Magnetic Resonance (NMR) is the physical phenomenon underlying magnetic resonance imaging (MRI). NMR occurs when nuclei with non-zero spin absorb and emit electromagnetic radiation whey the nuclei are placed in an external magnetic field. Most isotopes with an odd number of protons and/or neutrons such as hydrogen (^1H), carbon (^{13}C), and phosphorus (^{31}P) have a spin [**12Sandy**].

^1H is the most abundant isotope inside the body and is the commonly used nuclei in magnetic resonance imaging. Its properties such as a high gyro-magnetic ratio, and a non-zero spin, makes it suitable for conducting measurements that provides information about the structure of the scanned tissue. For interest readers we refer to the standard literature [**4and5Julio**]

2.1.1 Nuclear Spin and Magnetic Moment

Nuclei with an odd number of protons and/or neutrons possess a property called nuclear spin $\tilde{\mathbf{I}}$ of a nucleus with mass A . Since nuclei are not single entities, $\tilde{\mathbf{I}}$ is composed of the spins \vec{s}_i and the orbital angular momenta \vec{l}_i of the protons and neutrons in the nucleus which have a spin $s = \frac{1}{2}$. Its relation is described by:

$$\tilde{\mathbf{I}} = \sum_{i=1}^A \left(\vec{s}_i + \vec{l}_i \right). \quad (2.1)$$

Different nuclear spin configurations can be achieved depending on the number of protons and neutrons in the nucleus, with the quantum relations given by:

$$\hat{\mathbf{I}} |I, m\rangle = \hbar^2 I(I+1) |I, m\rangle \quad (2.2)$$

$$\hat{I}_z |I, m\rangle = \hbar m |I, m\rangle \quad (2.3)$$

with $\|\vec{\mathbf{I}}\| > 0$, using the spin operator $\hat{\mathbf{I}}$, m as the magnetic quantum number, and constant $\hbar = \frac{h}{2\pi}$ is the reduced Plank's constant 6.6×10^{-34} J s divided by 2π .

The nuclear spin can be related to a microscopic magnetic field which is formed by the charged nuclei rotating around its axis. The nuclear magnetic moment $\vec{\mu}$ is directly to the total spin angular momentum $\vec{\mathbf{I}}$:

$$\vec{\mu} = \gamma \vec{\mathbf{I}}, \quad (2.4)$$

where the proportionality constant γ , known as gyro-magnetic ratio, depends on the atomic nucleus.

To get the magnitude of $\vec{\mu}$ we use:

$$|\vec{\mu}| = \gamma \hbar \sqrt{I(I+1)}, \quad (2.5)$$

where I is the nuclear spin quantum number with values $I = 0, \frac{1}{2}, 1, \frac{3}{2}, \dots$. With the help of 2.1 we can derive:

- nuclei with odd A have half-integer I , e.g.: ^1H , ^{13}C .
- nuclei with even A and charge have $I = 0$, e.g.: ^{12}C , ^{16}O .
- nuclei with even A and odd charge have integer I , e.g.: ^2H , ^6Li , ^{14}N .

Hydrogen (^1H) has a relatively high gyro-magnetic ratio and is also one of the most abundant nuclei with non-zero spin in human tissue, which makes it perfect for MRI acquisitions.

2.1.2 Zeeman Effect

This magnetic moment points at a random direction in absence of a magnetic field, thus free spin systems have a spherical distribution of spin orientations due to the Boltzmann equation for thermal energy. In the presence of a magnetic field \vec{B}_0 , we can obtain the energy:

$$\mathcal{H} = -\vec{\mu} \cdot \vec{B}_0. \quad (2.6)$$

Without loss of generality we can assume that $\vec{B}_0 = B_z \vec{e}_z$. Then, the hamiltonian can be reformulated using [Equation 2.4](#) to:

$$\mathcal{H} = -\gamma I_z B_0. \quad (2.7)$$

Hence, the eigenstates of $\hat{\mathcal{H}}$ correspond to the eigenstates of \hat{I}_z , which in turn comprise of $2l + 1$ different values. Thus, we can denote the energy levels by:

$$E_m = -\gamma \hbar B_0 m, \quad -I \leq m \leq I, \quad (2.8)$$

which resembles an angular momentum $m\vec{u}$ precessing with the angular frequency $\gamma B_0 = \omega_L$, known as the *Larmor* frequency. [**Larmor**]

The resulting splitting of a single non-excited energy level into several new excited levels in the presence of an external magnetic field is called Zeeman effect depicted in [Figure ??](#). With the energy difference between energy levels:

$$\Delta E = |E_{m+1} - E_m| = \hbar \gamma B_0 = \hbar \omega_L. \quad (2.9)$$

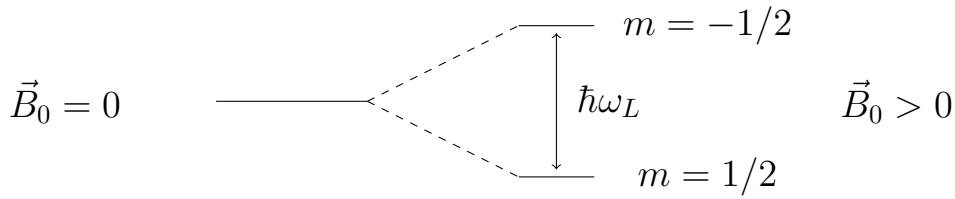


Figure 2.1: Zeeman effect on an energy level for a nucleus with nuclear spin $I = 1/2$. The energy difference between the levels is half the Larmor frequency ω_L multiplied by \hbar .

A spin system may have multiple resonant frequencies when presented with field inhomogeneities, shielding from neighboring spins, etc. This is called *chemical shift* which is described by a shielding constant δ :

$$\begin{aligned} B_0^{eff} &= B_0(1 - \delta) \\ \omega &= \omega_0 - \Delta\omega = \omega_0(1 - \delta) \end{aligned} \quad (2.10)$$

As an example, the hydrogen nuclei in a fat molecule CH_2 have a shielding constant of $\delta = 3.35$ ppm with respect to a proton in water.

The gyro-magnetic ratio of the proton (^1H) is $\gamma = 1.675\,221\,9 \times 10^8 \text{ s}^{-1} \text{ T}^{-1}$, which corresponds to a frequency of $f = \frac{\omega_L}{2\pi} = 127.732 \text{ MHz}$ for $B_0 = 3 \text{ T}$

2.1.3 Bulk Magnetization

The magnetic moments of N atomic nuclei sum up to a net bulk magnetization that describes the behaviour of the system:

$$\vec{M} = \sum_{i=1}^N \vec{\mu}_i. \quad (2.11)$$

Because in absence of an external magnetic field the nuclei in the human body are at thermal equilibrium, and the thermal energy is large compared to the energy of the non-excited spin state ($k_B T \gg \gamma \hbar B_0$) the occupation density of the spin states can be expressed using Boltzmann statistics. Hence, we can derive that the excess rate of spins pointing on a specific direction vs the spins pointing at the opposite direction can be described by the Boltzmann distribution:

$$\frac{N_{\uparrow}}{N_{\downarrow}} = \exp\left(\frac{\Delta E}{k_B T}\right). \quad (2.12)$$

where k_B is the Boltzmann constant.

Since $k_B T \gg \Delta E$ we can approximate to the first order [Equation 2.12](#). Thus denoting the excess spins N_s we derive the bulk magnetization as:

$$M_z^0 = \|\mathbf{M}\| \approx \frac{\gamma^2 \hbar^2 B_0 N_s}{4 k_B T} \quad (2.13)$$

At room temperature ($T = 300$ K), the number of spins in the up-state is almost equal to the number of spins in the down-state. Nevertheless, the high abundance of hydrogen in the human body generates sufficient bulk magnetization for imaging purposes.[\[aizada14\]](#).

2.1.4 Resonance and RF Excitation

When nuclei are subjected to an RF pulse at the Larmor frequency ($\omega_0 = \gamma B_0$), they absorb energy and are excited to a higher energy state. The resonance condition is met when the frequency of the RF pulse matches the Larmor frequency. This causes the net magnetization vector to tip away from the B_0 axis, creating transverse magnetization.

2.1.5 Relaxation Mechanisms

After the RF pulse is turned off, the excited nuclei return to their equilibrium state through relaxation processes:

- **T₁ (Longitudinal) Relaxation:** The recovery of longitudinal magnetization along the B_0 axis.
- **T₂ (Transverse) Relaxation:** The decay of transverse magnetization due to spin-spin interactions.

2.1.6 Chemical Shift

The chemical shift refers to the variation in resonance frequency of nuclei due to their chemical environment. This shift is crucial for distinguishing between water and fat signals in MRI, as the resonance frequency of fat protons is slightly lower than that of water protons.

2.2 MRI HARDWARE COMPONENTS

The main components of an MRI system include:

- **Static Magnetic Field:** Produced by a superconducting magnet, creating a strong and uniform field (B_0).
- **RF Coils:** Used for both transmitting the RF pulse and receiving the MR signal.
- **Gradient Coils:** Generate magnetic field gradients for spatial encoding.
- **Signal Reception:** The precessing transverse magnetization induces a voltage in the RF coils, which is detected and processed to form images.

2.3 SPATIAL ENCODING

Spatial encoding in MRI is achieved through the application of magnetic field gradients, which cause the Larmor frequency to vary with position.

2.3.1 *Slice Selection*

A gradient field applied along one axis (e.g., the z -axis) during RF excitation selectively excites a slice of tissue. The RF pulse is designed to match the Larmor frequency of the nuclei in the desired slice.

2.3.2 *Frequency Encoding*

Following slice selection, a gradient applied along a second axis (e.g., the x -axis) causes the resonance frequency to vary linearly with position. This frequency variation is used to encode spatial information.

2.3.3 *Phase Encoding*

A third gradient applied along a perpendicular axis (e.g., the y -axis) introduces a position-dependent phase shift. By incrementally changing the phase-encoding gradient, spatial information along this axis is encoded.

2.3.4 *k-Space and Image Reconstruction*

The combination of frequency and phase encoding gradients fills k-space, a matrix representing spatial frequencies. The MR image is reconstructed from the k-space data using the inverse Fourier transform.

WATER-FAT MRI

3.1 IMPORTANCE OF WATER-FAT SEPARATION

Water-fat separation in MRI is essential for assessing metabolic disorders such as obesity, metabolic syndrome, and type-2 diabetes. The technique provides insights into body fat distribution and helps derive biomarkers like the Proton Density Fat Fraction (PDFF).

3.2 CHEMICAL SHIFT ENCODING (CSE)

Chemical shift encoding (CSE) leverages the resonance frequency differences between water and fat protons to separate their signals. Multi-echo acquisitions are used to encode these differences, enabling the separation of water and fat signals into distinct images.

3.3 DIXON TECHNIQUES

The Dixon method involves acquiring images at multiple echo times to exploit the phase differences between water and fat signals. This technique can be applied both qualitatively, to suppress fat signals, and quantitatively, to measure fat concentration.

3.4 APPLICATIONS IN CLINICAL DIAGNOSTICS

Water-fat MRI techniques are widely used in clinical diagnostics to evaluate liver fat content, muscle composition, and other metabolic parameters. The separation of water and fat signals enhances the accuracy of these assessments.

CHALLENGES AND TECHNIQUES FOR ACCELERATION

4.1 MOTION ARTIFACTS

Motion artifacts arise from patient movement or physiological motion during MRI acquisition. These artifacts can degrade image quality and diagnostic accuracy.

4.2 RESPIRATORY TRIGGERING AND BREATH-HOLD TECHNIQUES

Respiratory triggering and breath-hold techniques are employed to mitigate motion artifacts. While effective, these methods can increase patient discomfort and extend scan times.

4.3 COMPRESSED SENSING (CS)

Compressed Sensing (CS) is a mathematical framework that accelerates MRI acquisition by reconstructing images from undersampled data.

4.3.1 *Principles of Compressed Sensing*

CS exploits the sparsity of MR images in a transform domain, enabling the reconstruction of high-quality images from fewer k-space samples.

4.3.2 *CS in MRI*

CS has been successfully applied to various MRI techniques, reducing scan times and improving image quality. The reconstruction process involves solving an optimization problem to recover the image from undersampled data.

4.3.3 *CS in Water-Fat MRI*

In water-fat MRI, CS can be used to accelerate the acquisition process by exploiting the redundancy in multi-echo data. This approach enhances the efficiency of water-fat separation and reduces scan times.

ADVANCED TECHNIQUES IN WATER-FAT MRI

5.1 FIELD MAPPING

Accurate field mapping is crucial for water-fat separation. Various algorithms have been developed to estimate the field map and correct for inhomogeneities.

5.2 IDEAL METHOD

The Iterative Decomposition of Water and Fat with Echo Asymmetry and Least-squares (IDEAL) method iteratively estimates water and fat signals, field map, and transverse relaxation rates.

5.3 GRAPH CUT ALGORITHMS

Graph cut algorithms provide an efficient approach for field map estimation, improving the accuracy of water-fat separation by minimizing artifacts.

5.4 CONCLUSION

MRI, leveraging the NMR phenomenon, offers unparalleled capabilities in both anatomical and functional imaging. The ongoing development of advanced techniques like CS in WF-MRI continues to enhance the efficiency and effectiveness of this imaging modality, making it invaluable in the clinical assessment of metabolic and other disorders.

Part III

APPENDIX

APPENDIX TEST

BIBLIOGRAPHY

- [1] In *Wikipedia*. 2024. URL: https://en.wikipedia.org/wiki/Magnetic_resonance_imaging.
- [2] T. Baum, C. Cordes, M. Dieckmeyer, S. Ruschke, D. Franz, H. Hauner, J. S. Kirschke, and D. C. Karampinos. “MR-based assessment of body fat distribution and characteristics.” In: *European Journal of Radiology* 85.8 (2016), pp. 1512–1518.
- [3] D. Franz, J. Syväri, D. Weidlich, T. Baum, E. J. Rummeny, and D. C. Karampinos. “Magnetic Resonance Imaging of Adipose Tissue in Metabolic Dysfunction.” In: *RöFo-Fortschritte auf dem Gebiet der Röntgenstrahlen und der bildgebenden Verfahren* 190.12 (2018), pp. 1121–1130.
- [4] Vikas Gulani and Nicole Seiberlich. “Quantitative MRI: Rationale and Challenges.” In: *Quantitative Magnetic Resonance Imaging*. Ed. by Nicole Seiberlich, Vikas Gulani, Fernando Calamante, Adrienne Campbell-Washburn, Mariya Doneva, Houchun Harry Hu, and Steven Sourbron. Vol. 1. Advances in Magnetic Resonance Technology and Applications. Academic Press, 2020, pp. xxxvii–li.
- [5] Mohammad Mansouri, Shima Aran, Harlan B. Harvey, Khalid W. Shaqdan, and Hani H. Abujudeh. “Rates of safety incident reporting in MRI in a large academic medical center.” In: *Journal of Magnetic Resonance Imaging* 43.4 (2016), pp. 998–1007.

COLOPHON

This document was typeset using the typographical look-and-feel `classicthesis` developed by André Miede and Ivo Pletikosić. The style was inspired by Robert Bringhurst’s seminal book on typography “*The Elements of Typographic Style*”. `classicthesis` is available for both \LaTeX and \LyX :

<https://bitbucket.org/amiede/classicthesis/>

Happy users of `classicthesis` usually send a real postcard to the author, a collection of postcards received so far is featured here:

<http://postcards.miede.de/>

Thank you very much for your feedback and contribution.